Mixed-Mode Fracture Tests for application of High-Strength Fiber-Reinforced Concrete for seismic isolation

S. Fukuoka & Y. Kitsutaka
Tokyo Metropolitan University, Japan

ABSTRACT: The mixed-mode fracture behavior of a mortar reinforced with vinylon fibers is investigated in this paper, in order to ascertain to what extent this material is suitable to be used in seismic-isolation devices. Since most of the studies on fracture mechanics of cement-based materials have regarded so far Mode I fracture, standard tests are limited to this type of behavior. However, an increasing number of researchers are investigating whether Mode II (shear fracture) exists and how its parameters can be measured. Starting from the assumption that Mode II exists (even if it is generally combined with Mode I), this study aims to investigate the fracture properties of the above-mentioned fiber-reinforced mortar, in order to assess its energy-absorption capability, in view of possible application to seismic devices. In this project, 4-point shear tests on notched prisms were carried out, and both the crack-mouth opening displacement (CMOD) and the crack sliding deformation (CSD) were measured by means of 2-axis LVDTs. Since the specimens were longitudinally confined by tightening two external steel bars, the favorable effect that the confinement has on mortar toughness was investigated as well. The evolution of the load versus CMOD and CSD was also monitored, to have information on mixed-mode fracture, as a step towards the still elusive formulation of appropriate constitutive laws for cementitious materials.

1 INTRODUCTION

Numerous research projects have been so far devoted to fracture in Mode I, in order to determinate the fracture parameters of various types of concrete and mortar, and to make proposals for standard tests (see for instance Bazant & Estenssoro, 1979; Arrea & Ingraffea, 1981; Bazant et al., 1984; Ingraffea & Panthaki, 1985; Rots & de Borst, 1987; Bazant & Pfeiffer, 1987; Swartz et al., 1988; Kaneko & Li, 1993). However several researchers are currently focusing their attention on the other fracture mode characterized by a slip – or slide - between the crack faces (Mode II), that brings in two interrelated problems: (1) whether the fracture process can evolve according to Mode II (without being accompanied by Mode I); and (2) how to evaluate the parameters of Mode II fracture. Both problems require experimental and analytical studies. In order to solve the second problem, achieving a state of pure shear is necessary, as well as forcing the propagation of a crack in such a way that K_{II} prevails over K_I. A specific test should be developed. The specimen should contain a flaw in the pure-shear region, in order to have a slide along the crack, and no – or very limited – opening. Unfortunately, concrete cracking in shear is generally characterized by mixed-mode fracture, because of the mixed boundary conditions. In this research project, the fracture behavior of a mortar reinforced with vinylon fibers is investigated, by testing a number of beams loaded in 4-point shear. The geometry of this test was first proposed by Iosipescu with a similar objective (shear strength of steel).

In 4-point shear tests, the specimens are designed in such a way that large shear stresses are accompanied by small bending stresses, and the two halves of each specimen do not undergo any mutual rotation. In Fig. 2 the geometry adopted by Arrea & Ingraffea (1981) is shown. The crack propagates from the tip of the notch along a curved path, with an initial angle $\alpha = 68°$ with respect to the horizontal axis.

Bazant & Pfeiffer (1987) used in their tests double-notched specimens (Fig. 1) characterized by a smaller horizontal distance between the point loads (0.167d) than in Arrea and Ingraffea's specimens (0.4d). In the former tests (Fig. 1), a macroscopic vertical fracture connecting the tips of the notches was observed. Such a fracture process was considered by Bazant & Pfeiffer as a demonstration that

Mode II fracture does exist. However, the authors concluded the the macro-fracture resulted from the cohalescence of many Mode-I micro-cracks at 45° to the horizontal axis, as shown in Fig. 1.

Within this context, the goals of this study are: (1) the presentation of a research program on a new testing procedure for mixed-mode fracture and on the measurement of mixed-mode fracture parameters; and (2) the investigation on the mixed-mode fracture behavior of the afore-mentioned fiber-reinforced mortar, with/without confinement, under both monotonic and cyclic loading.

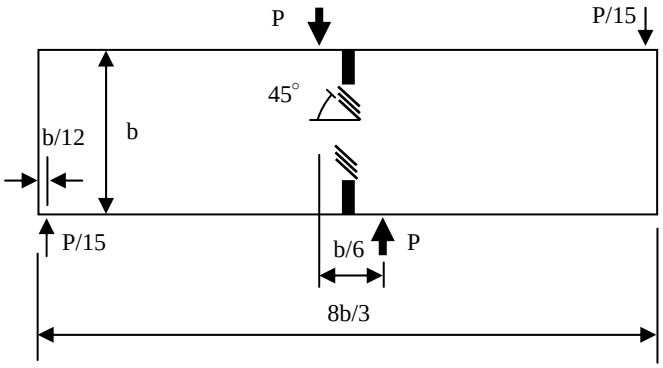

Fig. 1 Geometry of Bazant and Pfeiffer's specimens.

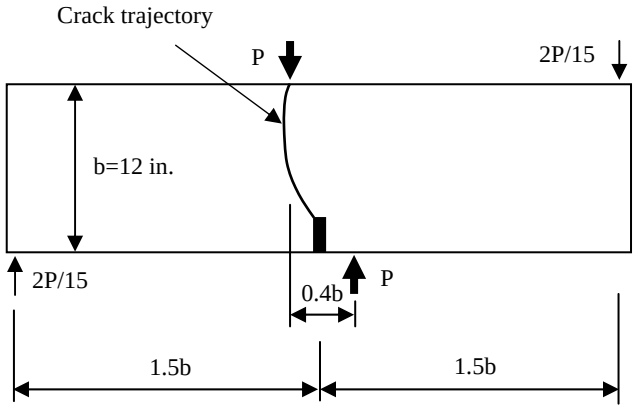

Fig. 2 Geometry of Arrea and Ingraffea's specimens.

2 EXPERIMENTAL PROGRAM

2.1 *Geometry of the specimens*

The mix design of the mortar and the physical properties of the fibers are given in Tables 1 and 2. The cylindrical compressive strength is close to 200 MPa and the maximum aggregate size is 3.5 mm. Prior to testing, the specimens (beams) were cured for 14 days at 20°C and 80% of R.H. The dimensions of the 8 beams (Fig. 3) were: w/d/l = 100/100/200 mm; the notch depth/section depth ratio was $a_0/w = 0.25$. A typical specimen is shown in Fig. 4 (mass m_g = 4.6 kg).

Table 1 – Mix Design.

Water / (Cement + Silica fume)	0.17
Fiber / (Cement + Silica fume)	1%
Water	187 kg/m^3
Cement	1029 kg/m^3
Silica fume	257 kg/m^3
Fine Aggregate	859 kg/m^3
Vinylon fiber: content/volume fraction	19 kg/m^3/1.5%
Superplasticizer	32.15 kg/m^3
Curing time	14 days

Table 2 – Physical properties of vinylon fibers.

Fiber Type	vinylon,VF1500
Length	30
m	m
Diameter	240×720 μm
Tensile Strength	882 MPa
Young's Modulus	29 GPa
Mass per unit volume	
1.3	0

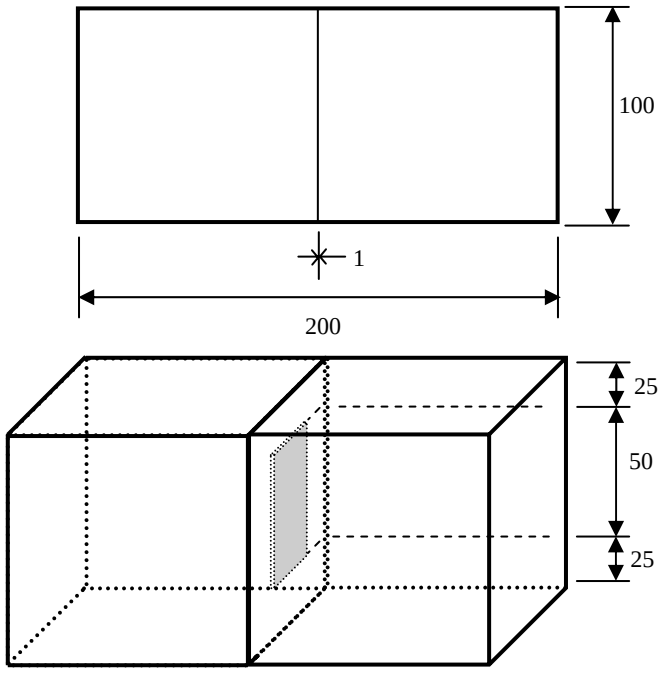

Fig. 3 Geometry of the specimens.

Fig. 4 View of an actual specimen.

2.2 *Test set-up*

A sketch of the test set-up, with the specimen, the point loads and the LVDTs is shown in Fig. 5. Between the rollers and the specimen thin metal strips are placed in order to avoid any friction. The distance between each couple of point loads is s = 100 mm. Two LVDTs are attached to either side of the specimen, at mid-height, and are connected to a data logger. The details of the two-axis LVDTs are given in Fig. 6.

All tests were displacement-controlled, by controlling the displacement rate of the crosshead of the press (0.1 mm/minute). The force exerted by the MTS press and the stroke were recorded every second.

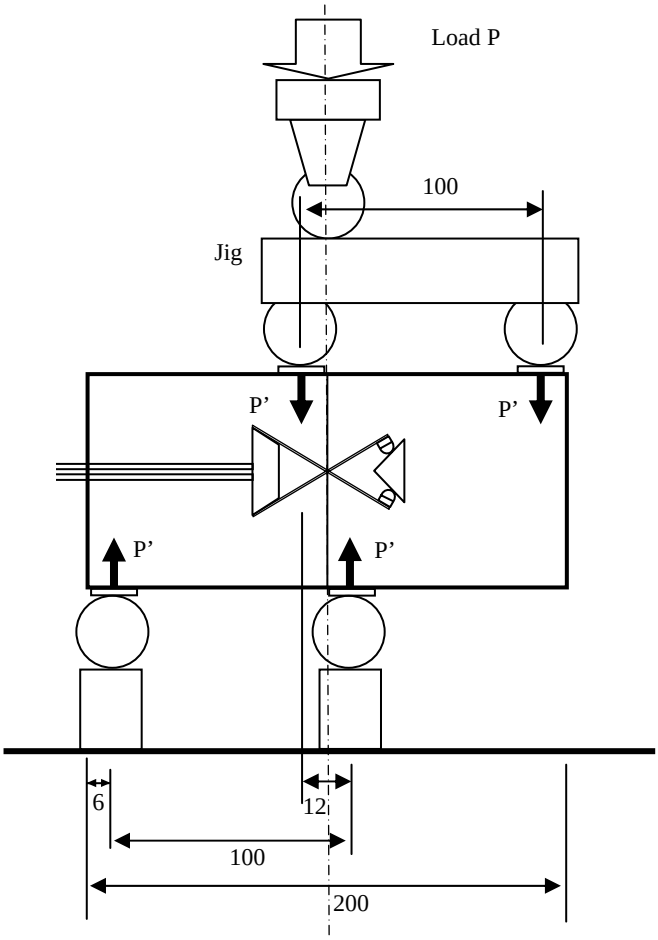

Fig. 5 Test set-up.

3 TEST SERIES

The fracture behavior of the mortar reinforced with vynilon fibers was investigated by performing 4 series of tests concerning notched prisms ("beams") loaded in 4-point shear. Each series consisted of 2 specimens:

Series 1: 2 unconfined specimens were tested under monotonic loading.

Series 2: same as in Series 1, but with confined specimens (see Figs. 7 and 8).

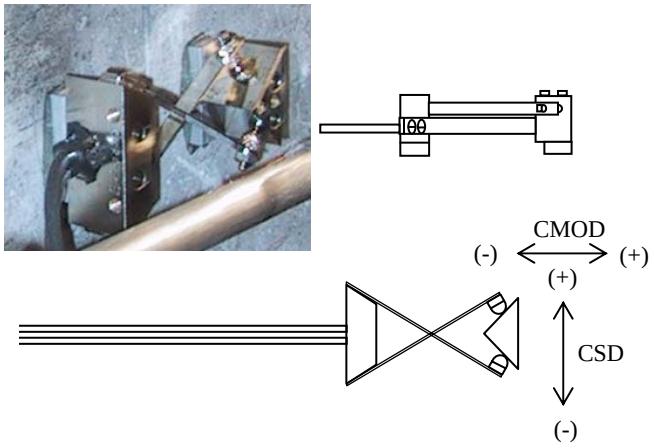

Fig. 6 Details of the 2-axis LVDTs.

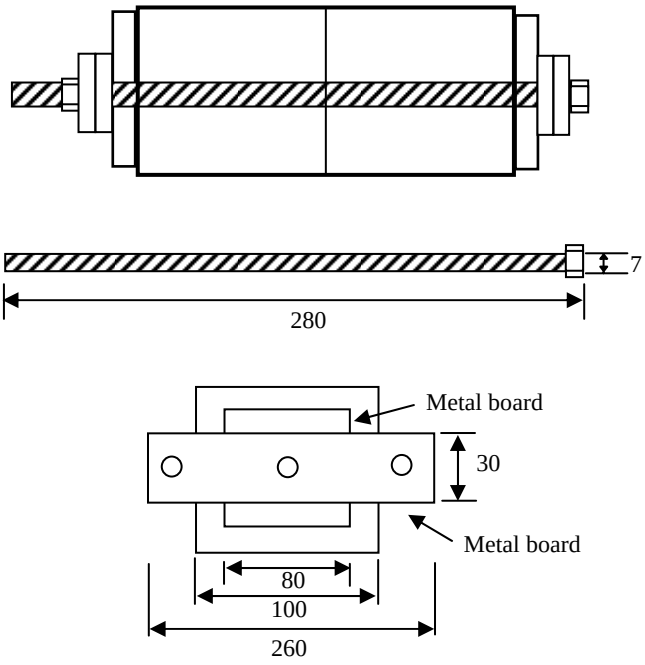

Fig. 7 Lateral view of the prismatic specimens (beams) provided with 2 confining bars (∅ = 7 mm).

Series 3: 2 unconfined specimens were tested under cyclic loading, to assess the bridging properties of vynilon fibers. During the first cycle each specimen was monotonically loaded up to the full cracking of the notched section, and then was unloaded. Subsequently, the two specimens were loaded and re-

loaded in two slightly-different ways. In the first specimen, the second and third cycles induced a ± 1 mm slide between the crack faces, while the fourth and fifth cycles induced a ± 2 mm slide. In the second specimen, the second and third cycles induced a ± 0.5 mm slide between the crack faces, while the fourth and fifth cycles induced a ± 1 mm slide.

Series 4: same as in Series 3, but with confined specimens.

4 RESULTS

The load-displacement curves of the 8 specimens tested in this project are shown in Figs. 9 and 10, 12 and 13, 15 and 16, 18 and 19. (LPD means Load-Point Displacement). As for the displacements, reference is made to the average CMOD and to the average CSD (average = mean of the two values measured on the front and back faces).

Test Series 1- Monotonic Loading – No Confinement

The force-displacement curves are plotted in Figs.9 and 10. The cracked surface of the 1st specimen is shown in Fig. 11. In both specimens the cracked surface was smooth. Looking at Fig. 9 one can observe that up to the peak load the force-CMOD curves are more extended than the force-CSD curves (Fig. 10), which means that fracture is caused by mixed-mode cracking, with small diagonal micro-cracks joining in a single vertical crack.

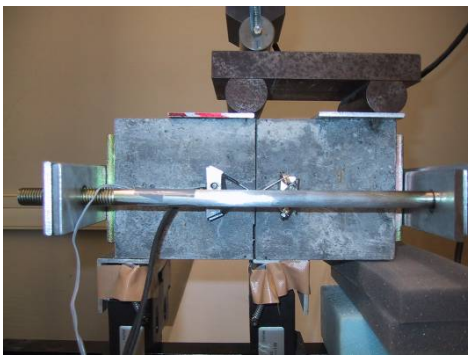

Fig. 8 Test set-up in Series 2 and 4.

Test series 2- Monotonic Loading – With Confinement

The force-displacement curves are plotted in Figs. 12 and 13. The cracked surface of the 1st specimen is shown in Fig. 14. In both specimens the fracture was caused by mixed-mode cracking, as in the previous case. However, because of the confinement the toughness of the material increased (more extended curves prior to the peak), the local angle α to the horizontal axis was smaller, and the cracked surface was not as smooth as in the previous case.

Test Series 3 – Cyclic Loading – No Confinement

The force-displacement curves are plotted in Figs.15 and 16. The cracked surface of the 1st specimen is shown in Fig. 17. Both specimens failed during the 3rd cycle, the former prior to reaching the maximum slip of 1 mm and the latter after reaching the same slip. Contrary to the specimens loaded monotonically, the local angle to the horizontal axis was partly positive and partly negative.

Test Series 4 – Cyclic Loading – With Confinement

The force-displacement curves are plotted in Figs. 18 and 19. The cracked surface of the 1st specimen is shown in Fig. 20. Local cracking was similar to that occurred in the previous tests. However, because of the confinement the toughness of the material increased, the local angle α to the horizontal axis was smaller, and the cracked surface was not as smooth as in the previous case.

As for the confining action, the relationship between the stress in each restraining bar and the applied load is plotted in Figs. 21 and 22. Note that in both Series 2 and Series 4 the initial confinement ("active" confinement) was very small, since the objective of the tests was to investigate crack cohesion due to the fibers, rather than the direct effects of the confinement.

In Series 2 (Fig.21), the initial stresses in the confining bars were similar (mean value 4.3 MPa) and the total initial confining force was close to 330N (compressive stress acting on the notched section = 0.13 MPa).

In Series 4 (Fig.22), the initial stresses in the confining bars were different (0.8 MPa in the 1st test and 8.8 MPa in the 2nd test) and the total initial confining forces were 62 N and 677 N respectively.

Figs.21 and 22 show also that – because of shear-induced crack dilatancy – the stresses in the confining bars started increasing above 20-30 kN in the tests of Series 2 and above 25-35 kN in the tests of Series 4 ("passive" confinement). However, the lar-

ger the confinement, the smaller the effects of crack dilatancy (2nd test in both Series 2 and 4).

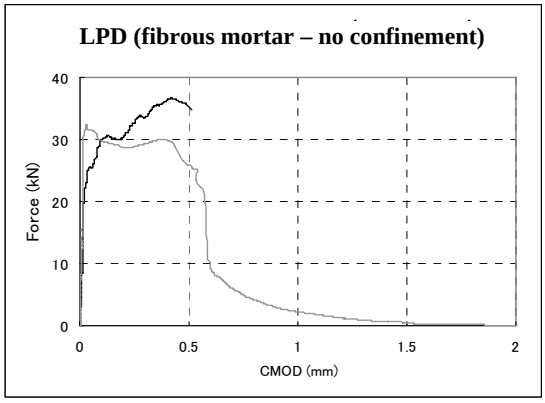

Fig. 9 Load-CMOD curves in Series 1.

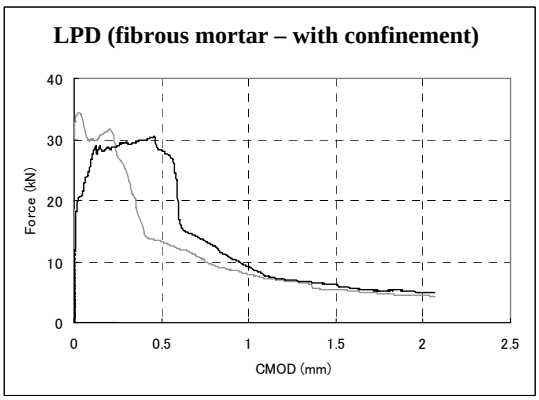

Fig. 10 Load-CSD curves in Series 1.

Fig. 11 Typical fracture in Series 1.

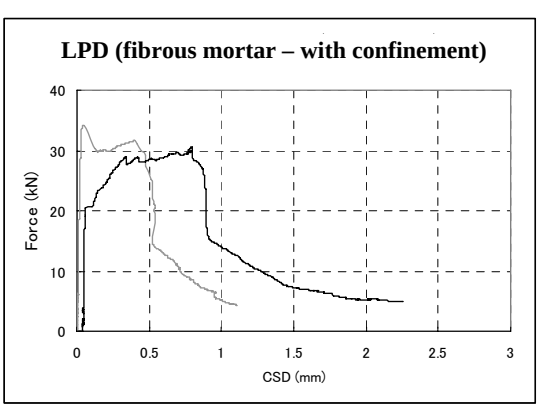

Fig. 12 Load-CMOD curves in Series 2.

Fig. 13 Load-CSD curves in Series 2.

Fig. 14 Typical fracture in Series 2.

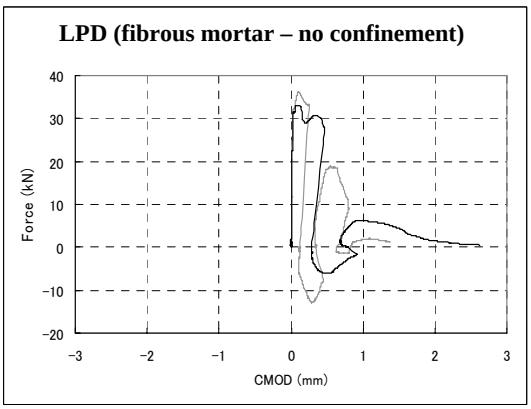

Fig. 15 Load-CMOD curves in Series 3.

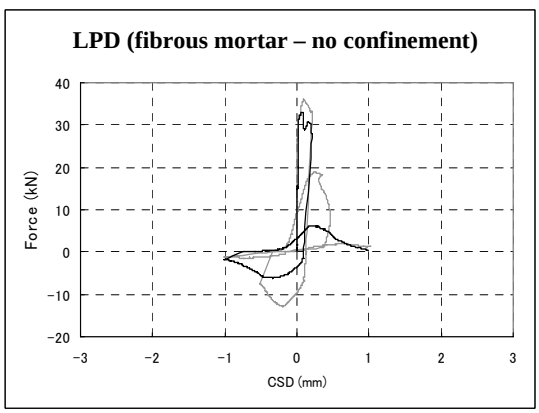

Fig. 16 Load-CSD curves in Series 3.

Fig. 17 Typical fracture in Series 3.

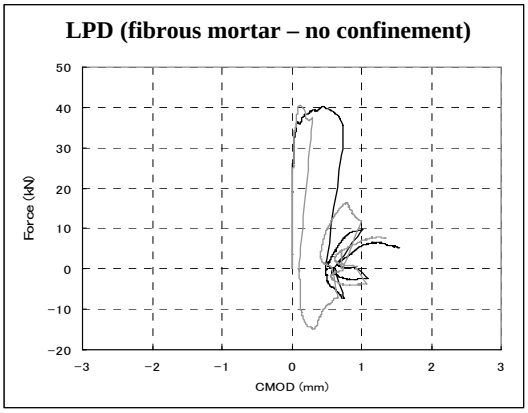

Fig. 18 Load-CMOD curves in Series 4.

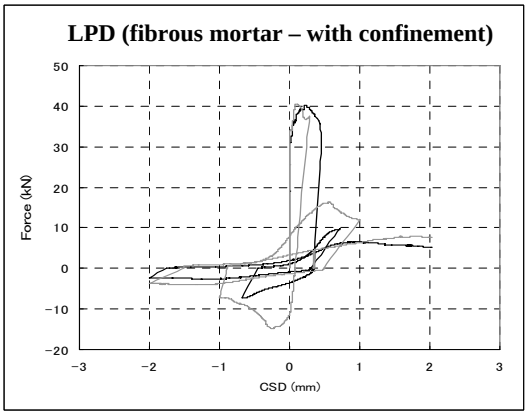

Fig. 19 Load-CSD curves in Series 4.

Fig. 20 Typical fracture in Series 4.

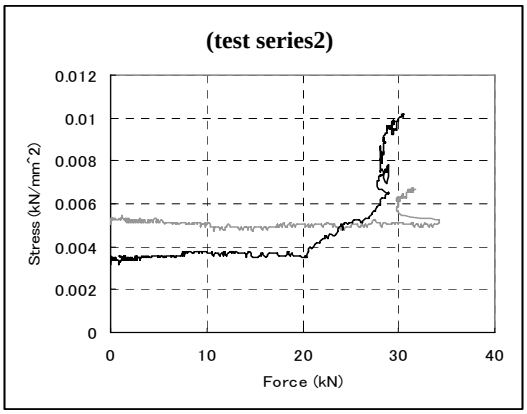

Fig. 21 Plot of the stress in the confining bars, as a function of the applied load (Test Series 2).

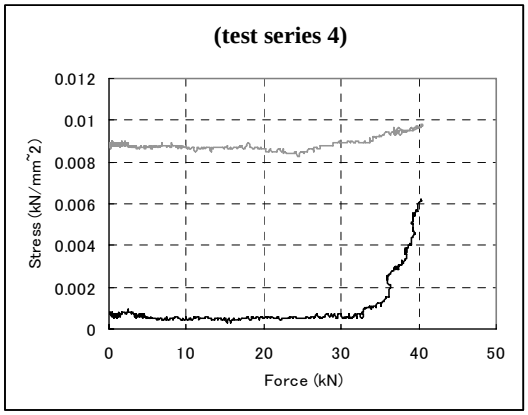

Fig. 22 Plot of the stress in the confining bars, as a function of the applied load (Test Series 4).

5 CONCLUSIONS

1. In all fiber-reinforced specimens – and particularly in the unconfined specimens – the shear-induced crack results from the cohalescence of local diagonal micro-cracking.
2. In the confined specimens, both the toughness and the strength markedly increase.
3. Introducing vinylon fibers in the mix design markedly softens the post-peak behavior.
4. In confined specimens, the interface of the shear-induced crack is rather rough, since combining the shear force and the longitudinal confinement tends to diminish the local angle of the micro-cracks to the horizontal axis.
5. The load-CMOD curves exhibit a more extended plateau close to the peak load, than the load-CSD curves, which means that Mode I tends to prevail over Mode II; however, the slide at the crack interface is not at all negligible compared to crack opening; the fracture is characterized by mixed

mode, with the final crack resulting from the coalescence of many diagonal micro-cracks, as mentioned in point 1.

6. The test procedure proposed in this paper may be useful to evaluate the fracture properties in mixed-mode fracture in cementitious composites.
7. The results concerning both CMOD and CSD – under sustained and cyclic loading – give information useful to the formulation of the constitutive laws for mixed-mode fracture.

NOTATION

a_0 = notch depth;
w, d, *l*, m_g = width, depth, length and mass of each specimen (beam);
s = distance between the two point loads acting at the bottom and the top of each specimen;
CSD = crack sliding displacement;
CMOD = crack-mouth opening displacement;
K_I = stress intensity factor in Mode I;
K_{II} = stress intensity factor in Mode II;
LPD = load-point displacement;
α = angle of the crack to the horizontal axis.

ACKNOWLEDGEMENTS

This research project was financially supported by Tokyo Metropolitan University in 2006, within the Grant-in-Aid Program for Scientific Research launched by the Japanese Ministry of Education, Science, Sports and Culture, and spanning over the period 2005-07. The cooperation by Dr. Tamura Masaki – Research Associate at Tokyo Metropolitan University – is also gratefully acknowledged.

REFERENCES

Swartz S.E., Lu L.W. & Tang L.D. 1988. Mixed-mode fracture toughness testing of concrete beams in three-point bending. Materials and Structures 1998, 21, 33-40.

Bazant Z.P. & Pfeiffer P.A. 1987. Shear Fracture Tests of Concrete. Materiaux et Constructions 19, 111-121.

Kaneko Y. & Li V.C. 1993. Fracture Behavior of Shear Key Structures with a Softening Process Zone. International Journal of Fracture 59, 345-360.

Rots J.G. & de Borst R. 1987. Analysis of Mixed-Mode Fracture in Concrete. Journal of Engineering Mechanics, Vol.113, No. 11

Arrea, M. & Ingraffea, A.R., 1981. Mixed-Mode Crack Propagation in Mortar and Concrete. Rep. 81-13, Dept. of Structure. Eng.,Cornell University (N.Y., USA).

Ingraffea, A.R. & Panthaki, M.J., 1985. Analysis of Shear Fracture Tests of Concrete Beams. Proc. U.S. – Japan Seminar on Finite Element Analysis of Reinforced-Concrete Structures, Tokyo, May 21-24, 71-91

Bazant Z.P. & Estenssoro L.F. 1979. Surface Singularity and Crack Propagation. Int. J. of Solids and Structrures, Vol.15, 405-426, Addendum Vol.16, 479-481.

Bazant Z.P., Kim J.K. & Pfeiffer P.A. 1984. Determination of Nonlinear Fracture Parameters from Size Effect Tests. NATO Advanced Research Workshop on Application of Fracture Mechanics to Cementitious Composites, ed. by S.P.Shah, held at Northwestern University (Evanston, Illinois, USA), Sept. 4- 7, 143-169